Available online at www.sciencedirect.com

ScienceDirect

Procedia Manufacturing 39 (2019) 484–492

Procedia MANUFACTURING

www.elsevier.com/locate/procedia

25th International Conference on Production Research Manufacturing Innovation:
Cyber Physical Manufacturing
August 9-14, 2019 | Chicago, Illinois (USA)

Automatic Feature-Based Point Cloud Alignment and Inspection

Yu Jin, Haitao Liao, Harry Pierson*

Industrial Engineering, University of Arkansas, Fayetteville, AR,72701, USA

Abstract

3D scanning is a non-contact geometric inspection technique that has potential applications in many industrial sectors. Compared to coordinate measuring machines, 3D scanning is able to acquire high-density sampling of an entire part in a relatively short time without fixturing. In practice, point clouds, which are the output of 3D scanning, must be aligned with the base-truth CAD model before calculating the point-wise deviation. Existing methods accomplish this task by determining the optimal transformation that maximizes the overlap between the point cloud and base-truth CAD model. However, these methods do not consider the problem from a geometric dimensioning and tolerancing (GD&T) perspective. Specifically, dimensional errors are not quantified in reference to the established datum features. In this work, a new scheme is proposed to automatically align the datum features of 2D shapes based on point clouds via a polar coordinate representation. From the result of the new alignment scheme, the point-wise deviation is evaluated through the deviation distribution to differentiate manufacturing and measurement errors. The proposed scheme is applied in three case studies, in which the sample shapes to be inspected are generated by adding random errors to their nominal models to mimic measurement errors in physical experiments. The result illustrates the effectiveness and efficiency of the proposed scheme in automatic shape alignment based on datum features and in subsequent detection of point-wise deviation.

Keywords: Geometric Inspection; 3D scanning; Additive Manufacturing

* Corresponding author. Tel.: +1-479-575-6034; fax: +1-479-575-8431.
E-mail address: hapierso@uark.edu

10.1016/j.promfg.2020.01.405

1. Introduction

With the development of modern manufacturing techniques, the dimensional accuracy and precision measuring become indispensable in many complex and flexible environments. The coordinate measuring machine (CMM), as a traditional measuring tool, might not be able to perform well in inspecting a complex-shaped part, measuring in-process subassemblies, or inspecting the shape of a layer in additive manufacturing (AM). 3D scanning, as one of the non-contact geometrical inspection techniques, has now been widely adopted in many industrial sectors to tackle the inspection requirements which may not be fulfilled by the coordinate measuring machine (CMM).

Compared to CMM, 3D scanning can provide a high-density sampling of an entire part in a relatively short time without fixturing. Especially in the context of in-situ quality inspection and monitoring, a 3D scanner is able to provide an instant output of the current layer or working surface. The shape of the current layer or working surface is described by a two-dimensional point cloud obtained from the 3D scanning. In practice, the point cloud must be aligned with the base-truth CAD model before dimensional accuracy evaluation.

Previous studies suggest several alignment methods including best fit alignment, degree of freedom (DOF) alignment and feature-based alignment [1]. These methods are common options provided in point cloud processing software. In general, these methods are implemented by applying a simple singular value decomposition, principal component analysis-based registration, or Iterative Closest Point (ICP) algorithm [2]. The main idea these methods is to perform least-square fitting to find the optimal rigid transformation that minimizes the sum of the squared 3D distances between the measured alignment points and their target reference points [3]. The best fit alignment is non-specific alignment, usually based in ICP, via global optimization without considering the functionality and importance of points in different areas. For instance, Zheng et al. [4] and Zhang et al. [5] adopted best-fitting methods to align worn turbine blades to the nominal CAD model for damage detection and reconstruction. The DOF alignment is also called “3-2-1 Alignment”, which aligns the scanned data to the reference by gradually removing degrees of freedom of movement. For instance, Avagyan et al. [6] proposed an alignment adjustment method based on a viewpoint of estimating the “degree of alignment” for the given pair of surfaces. Feature-based alignment is also based on the ICP framework, but it is a more advanced method that is able to align point clouds by using those points associated with some pre-specified features. Li and Guskov [7] used signature vectors of a set of salient features with scale-space representation to achieve approximate alignment. Hong-Seok and Mani [8] applied a feature-based ICP to align a point cloud with the corresponding CAD model for defect detection. However, these methods did not consider features from a GD&T perspective. In recent years, some commercial software packages have started to adopt feature-based ICP alignment. For instance, BuildIT Construction [9] offers an alignment option based on the given feature/datum. Nevertheless, it usually requires a global least-square fitting before local alignment based on selected features. Moreover, the points associated with these features are usually selected manually by users.

In this work, a new scheme is proposed to automatically align the datum features of 2D shapes based on the point clouds via a polar coordinate representation. This scheme is motivated by the phase correction [10] applied in image registration. The main idea of phase correction is to find the phase shift by representing the original image in the polar coordinate system. The advantage of this scheme is that it can directly align the reference shape to the sample point cloud without a rough pre-alignment or manual intervention. More importantly, the point-wise deviation can be evaluated through the deviation profile to differentiate manufacturing, measurement, and alignment errors.

2. Method

2.1. Overview

Throughout this paper, the in-plane (X-Y) geometric shape deviation is considered for inspection, which is especially essential for online monitoring in AM processes. The shape can be represented with a two-dimensional point cloud, which can be obtained from a thin layer of the 3D point cloud, or tracing points along the boundary of the shape obtained by a top-view scan. Therefore, it is assumed that the scanned part and CAD model have been aligned in Z direction. The point cloud inspection process is summarized in Fig. 1, which is conducted in three major

steps. First, transform both the reference and sample point clouds from the Cartesian coordinate system (CCS) to a polar coordinate system (PCS) and represent the points in a form of polar functional representation. The functional representation of a point cloud is called a *profile*. Second, align the profile of the two point clouds by mapping the datum segment of the reference profile to the sample profile. Third, quantify the alignment error and point-wise deviation of the sample shape. The technical details of each step are illustrated as follows.

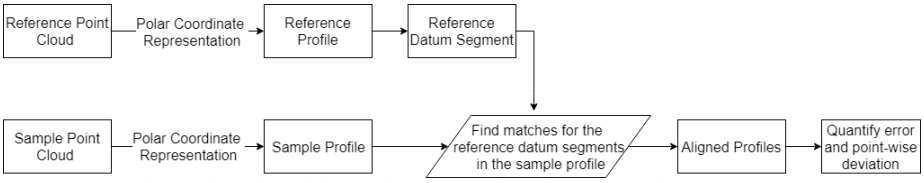

Fig. 1. Flow chart of feature-based point cloud alignment and inspection.

2.2. Polar Functional Representation of the Point Cloud

Given a point (x, y) in the given 2D point cloud, the corresponding polar coordinate can be obtained by calculating the angle θ and radius ρ with respect to the centroid of the 2D shape. Let $(\boldsymbol{\Theta}, \mathbf{P})$ denote the point cloud represented with polar coordinates. The range of $\theta \in \boldsymbol{\Theta}$ should be within $[-\pi, \pi]$, and the radius $\rho \in \mathbf{P}$ should be normalized into a range of $[0,1]$ to eliminate the scale effect. The polar functional representation, or *profile*, is a piecewise polynomial function estimated based on the polar coordinates $(\boldsymbol{\Theta}, \mathbf{P})$. The radius $\rho(\theta)$ at any $\theta \in \boldsymbol{\Theta}$ can be calculated based on the piecewise polynomial function. An example is given in Fig. 2 to represent the 2D point cloud in CCS, PCS, and in a form of profile.

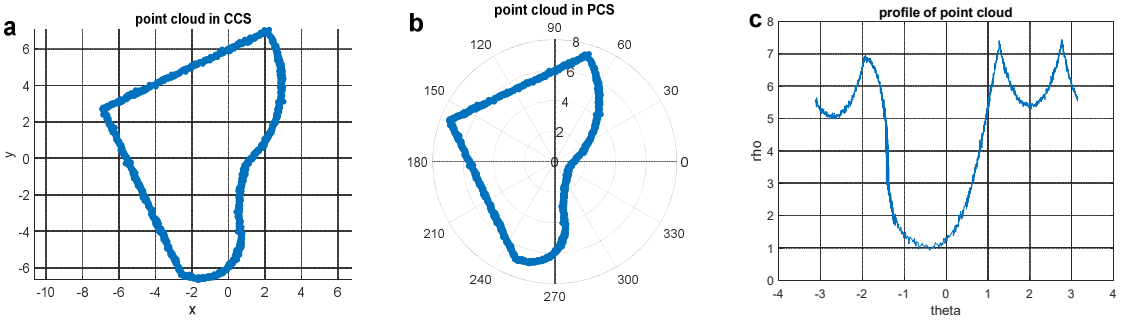

Fig. 2. (a) 2D point cloud in CCS; (b) 2D point cloud in PCS; (c) the profile of the point cloud.

A profile is constructed for the reference point cloud and sample point cloud, respectively. Of note, in order to establish point-wise correspondence between the reference point cloud and sample point cloud, the same query set $\boldsymbol{\Theta}$ is applied on both reference and sample profile to generate the corresponding radii. For any $\theta \in \boldsymbol{\Theta}$, the reference radius is denoted as $\rho^{(r)}(\theta)$ and the observed radius in the sample is denoted as $\rho^{(s)}(\theta)$.

2.3. Alignment based on the Datum Feature

The datum feature is recognized as a segment in the reference profile. It can be easily identified based on the points associated with the datum features in the reference point cloud (see Fig. 4), which is pre-known and defined from the engineers' perspective in the design stage. The proposed alignment method is able to align the reference profile to the sample profile by searching the best matches for the datum segment. Given a datum segment in the reference profile, the alignment process can be implemented with three steps. Case 1 in section 3 provides an example to illustrate the process.

First, find the best match for the reference datum segment in the sample profile by similarity search [11]. Different cost/distance measurements can be applied to evaluate the similarity. The similarity search algorithm will return the start and end θ's indices of the best matched segment in the sample profile (see Fig. 5b). It is worth noting that there are two special cases that users might encounter in searching for the best match.

- If the datum segment is not a continuous piece in one of the profiles, then it is possible that no best match can be found in the sample profile. To deal with it, the algorithm will extend the original sample profile with an additional cycle to ensure that at least one best match can be found for the reference datum segment.
- If a part has multiple identical datum features, the algorithm allows for returning the position of multiple matches for the reference datum. The ambiguity can be eliminated by finding the alignment that minimizes the deviation. An example with multiple identical datums is given in section 3.2.

Second, calculate the shift $\Delta\theta$ that requires moving the reference datum segment to the position of its best match. Let $\theta_{datum}^{(s)}$ denote the start position of the best match found in the extended sample profile and $\theta_{datum}^{(r)}$ denote the original start point of the reference datum in the reference profile. The datum segment shift $\Delta\theta = \theta_{datum}^{(s)} - \theta_{datum}^{(r)}$ is the distance required to move the reference datum segment from its original position to the position of the best match along the θ-axis (see Fig. 5c). The sign of $\Delta\theta$ indicates the direction of movement with regard to the original position.

Third, align the reference profile to an extended sample profile based on the datum segment shift (see Fig. 6a). The reference profile is shifted by $\Delta\theta$ together with the datum segment. If the shift is negative, the sample profile is extended with an additional cycle on the left; otherwise, the sample profile is extended with one cycle on the right. Thus, all points in the reference profile after the shift can find their correspondence in the extended sample profile. The aligned sample profile is the segment overlapped with the aligned reference profile in the extended sample profile.

2.4. Error Evaluation

Based on the aligned reference and sample profile with aligned query set $\mathbf{\Theta_A}$, the deviation at any $\theta \in \mathbf{\Theta_A}$ can be calculated by

$$\Delta\rho(\theta) = \rho^{(s)}(\theta) - \rho^{(r)}(\theta) \tag{1}$$

The deviated radius $\Delta\rho(\theta)$ is an accumulative error made by considering the total effects of systematic error, alignment error, and other random errors. Among all these error terms, the systematic error is the main one to be monitored for identifying the abnormalities resulting from the process or design errors. This type of error can be distinguished from the random error using a multi-resolution alignment methodology [12]. The alignment error is associated with the accuracy and precision of the datum feature. It can be evaluated by the root mean squared error calculated based on the aligned datum segments. The alignment error e_a can be calculated by

$$e_a = \sqrt{\frac{\sum_{\theta \in \mathbf{\Theta_{ADatum}}} \left(\rho^{(s)}(\theta) - \rho^{(r)}(\theta)\right)^2}{|\mathbf{\Theta_{ADatum}}|}} \tag{2}$$

where $\mathbf{\Theta_{ADatum}}$ is a query set associated with the aligned datum segment. A large alignment error may indicate poor datum quality. To improve the alignment performance, one can either (1) apply a global least-square fit prior to the local datum feature alignment, or (2) report the nonconformity of datum to the users for future adjustment.

3. Case Studies

The proposed inspection framework is applied on three case studies. The first case is used for demonstrating the inspection process. The second case is presented to illustrate how the proposed scheme can be applied to deal with special shapes which have symmetric or identical datums. The third case is designed to show the capability of the proposed scheme in aligning and inspecting free-form shapes. To illustrate these cases, three nominal shapes shown in Fig. 3 are considered. All the sample shapes to be inspected in the three case studies are generated by adding random errors to their nominal model to simulate the measurement variations in physical experiments. In the first and third case, some deviation is added to a certain area of the shape to simulate the symmetric error that might be observed in real production process. All three cases studies are implemented with Matlab with Intel Core i7 CPU.

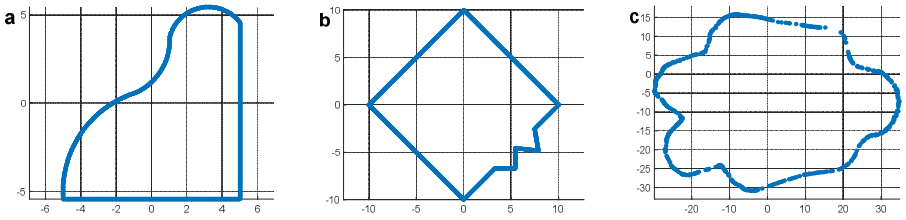

Fig. 3. (a) Case 1; (b) Case 2; (c) Case 3.

3.1. Case 1

In the first case study, a defective sample shape shown in Fig. 4a is provided to illustrate procedures of the proposed inspection scheme. Since the sample shape has not been aligned with the reference shape, the edge pointed out in Fig. 4a is considered the datum feature for alignment. Both reference and sample point clouds are transformed from CCS to PCS by considering the geometric center as the origin (Fig. 4b). Then each polar point cloud is presented as a profile where the datum segment of the reference profile is highlighted in Fig. 4c.

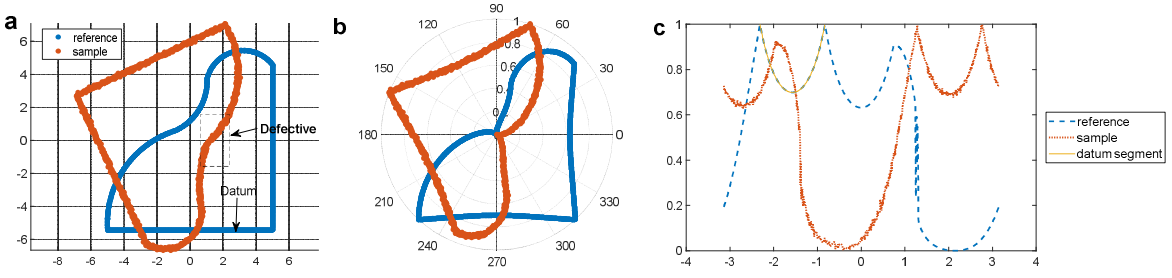

Fig. 4. (a) point clouds in CCS; (b) normalized point clouds in PCS; (c) polar profiles of point clouds.

As shown in Fig. 5, a best match for the datum segment is found in the sample profile. The start and end position shown in the figure are the start and stop θ's indices of the matched segments in the query set $\boldsymbol{\Theta}$. Then the distance or the shift $\Delta\theta$ between the reference datum segment and the best matched segment in the sample profile can be obtained. In this case, the reference profile needs to move toward the right with $\Delta\theta = 3.588$ radians.

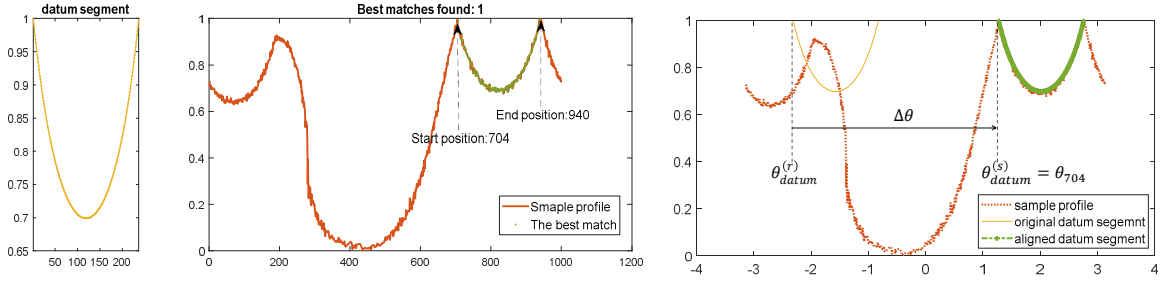

Fig. 5. Find the best match of datum segments and calculate the θ shift.

To obtain the segment overlapped with the aligned reference profile, the sample profile is extended with one more cycle on the right (Fig. 6a). The alignment result is also demonstrated in the original CCS (Fig. 6b). It is observed that the sample shape has a defective area, which can also be identified in the point-wise deviation profile as shown in Fig.

7. In practice, a specification limit defined by the users can be applied on the deviation profile to find the defective area of the sample shape.

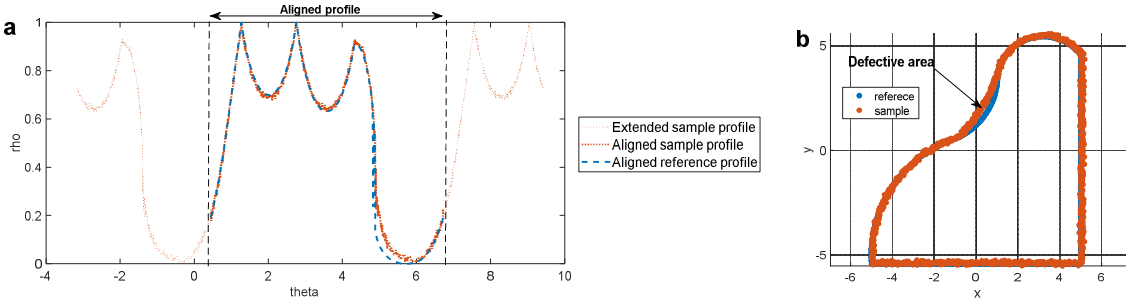

Fig. 6. (a) The aligned profiles; (b) aligned point cloud.

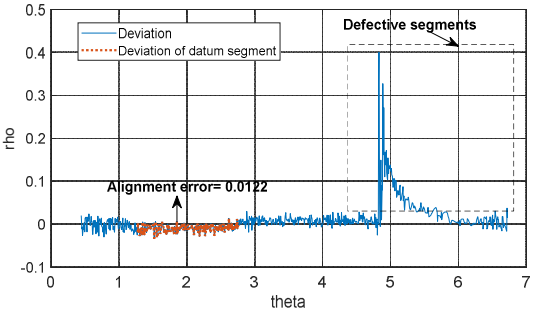

Fig. 7. Point-wise deviation profile of the given sample in case 1.

3.2. Case 2

The second case study was conducted to illustrate how to apply the proposed scheme to eliminate the ambiguity if multiple alignments exist. The shape of the second case has three identical edges. As shown in Fig. 8, if considering one edge as the datum feature, three best matches can be found in the sample profile for the datum segment. Therefore, three different shifts are applied to align the reference profile to the sample profile. The alignment result based on the three shifts is demonstrated in Fig. 9. The best alignment among the three is determined based on the deviation profile. It is observed in Fig. 9 that the best alignment among the three is the third one, which achieves the minimum overall deviation.

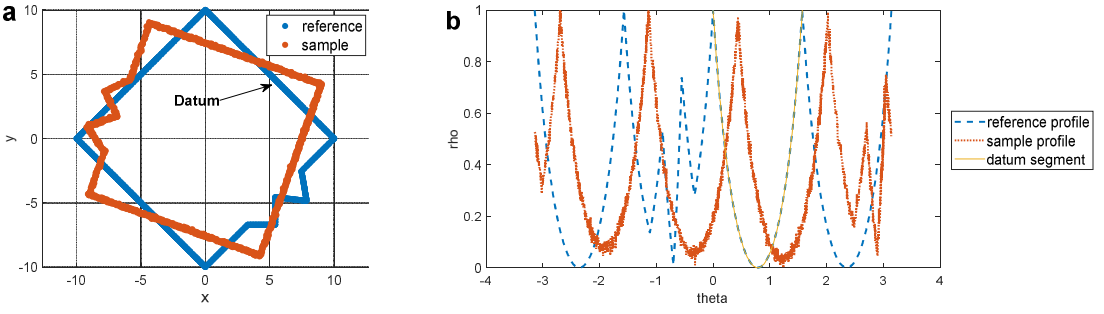

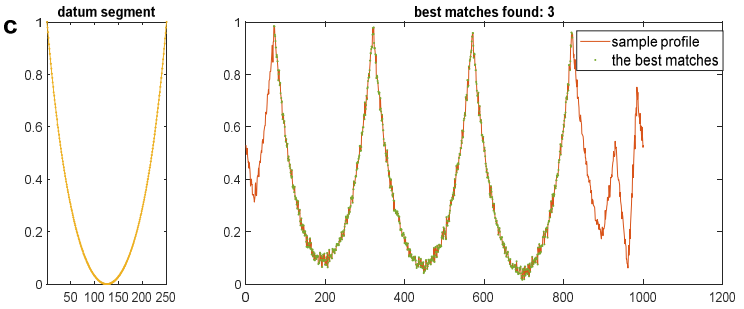

Fig. 8. (a) Overview of sample and reference shape of case 2; (b) sample and reference profile; (c) find best matches of the datum segment.

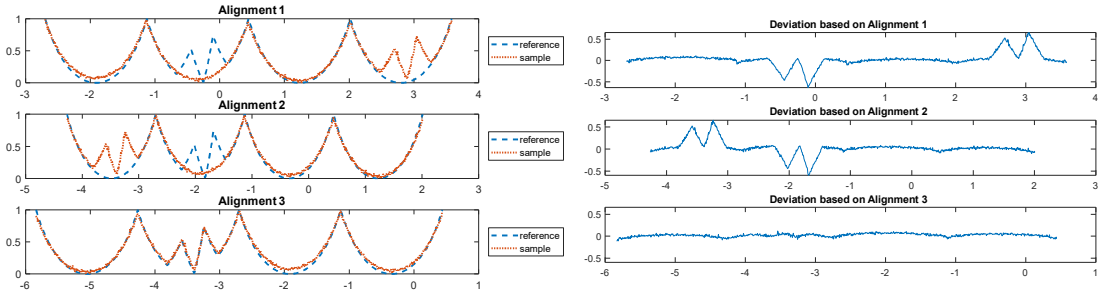

Fig. 9. Deviation evaluation based on different alignment results.

3.3. Case 3

The third case illustrates the potential application of the proposed scheme in free-form shape inspection. The shape used in this case is the 10th layer of the Stanford bunny model [13] that is obtained in the process of 3D printing (see Fig. 10). For a free-form shape, the datum is not necessarily associated with a GD&T feature and can be any complex/non-parametric features defined by the user. For example, in the given layer of the bunny model, the "tail" of the bunny, which is circled out in Fig. 11(a), is considered the datum. The two "feet" of the bunny are known as the defective areas.

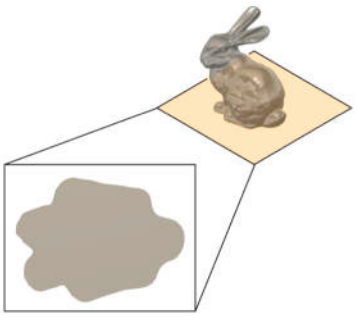

Fig. 10. The 10th layer of the Stanford bunny.

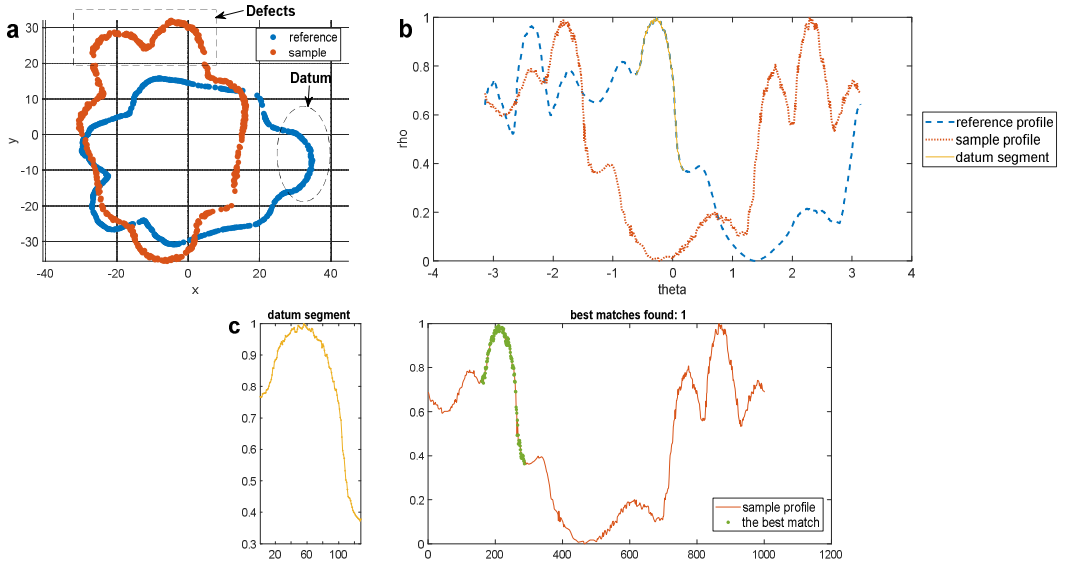

Fig. 11. (a) Overview of sample and reference shape of case 3; (b) sample and reference profile; (c) find the best match of the datum segment.

As shown in Fig. 11(b) and (c), the reference datum segment found one matched segment in the sample profile. After aligning the reference profile to the sample profile based on the position of the matched segment, the deviation profile and the alignment error are obtained in Fig. 12. Large deviations are observed at the segments which are associated with the pre-known defective area.

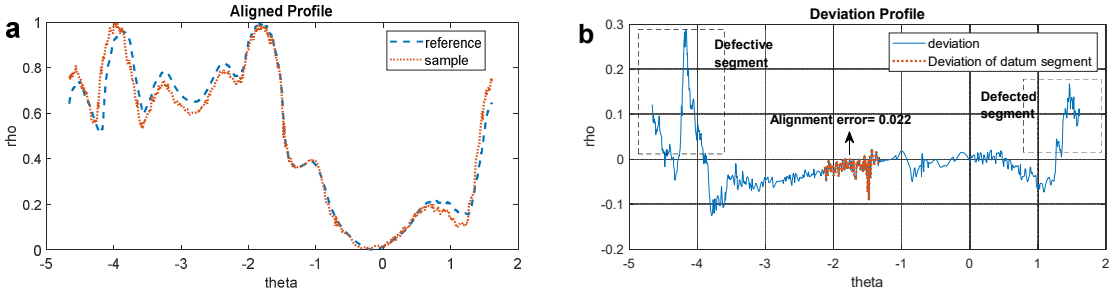

Fig. 12. (a) Alignment result of case 3; (b) deviation profile of the given sample in case 3.

4. Conclusions

This paper proposed a new alignment and inspection scheme based on a polar functional representation. The alignment method is based on the datum feature, which can automatically align two shapes without a rough global least-square fitting. Based on the result of the proposed scheme, the point-wise deviation can be evaluated through the deviation profile with polar coordinates to differentiate manufacturing, measurement, and alignment errors. The proposed scheme is applied to three case studies to evaluate the effectiveness and efficiency even in inspecting shapes that have symmetric and identical datums, or freeform features. In our future work, the proposed scheme will be applied to more complex shapes with internal features.

References

[1] P.C. Hammett, L. M. Garcia-Guzman, W. G. Steven, and T.W. Patrick, Quantifying alignment effects in 3D coordinate measurement., University of Michigan Transportation Research Institute, Manufacturing Validation Solutions, LLC, 22 (2009).
[2] B. Bellekens, V. Spruyt, R. Berkvens, M, Weyn. A survey of rigid 3D point cloud registration algorithms, AMBIENT 2014: the Fourth International Conference on Ambieant Computing, Applications, Services and Technologies, (2014) 8–13.
[3] P.J. Besl and N.D. McKay, Method for registration of 3-D shapes. Sensor Fusion IV: Control Paradigms and Data Structures, 1611(1992)586–607.
[4] J. Zheng, Z. Li, and X. Chen, Worn area modeling for automating the repair of turbine blades, The International Journal of Advanced Manufacturing Technology, 29.9-10 (2006) 1062-1067.
[5] X. Zhang, W. Li, and F. Liou, Damage detection and reconstruction algorithm in repairing compressor blade by direct metal deposition, The International Journal of Advanced Manufacturing Technology, 95.5-8 (2018) 2393-2404.
[6] V. Avagyan, A. Zakarian, and P. Mohanty, Scanned three-dimensional model matching and comparison algorithms for manufacturing applications, Journal of Manufacturing Science and Engineering 129.1 (2007) 190-201.
[7] X. Li, and I. Guskov, Multiscale features for approximate alignment of point-based surfaces, Symposium on geometry processing, 255(2005) 217.
[8] P. Hong-Seok, and T. U. Mani, Development of an inspection system for defect detection in pressed parts using laser scanned data, Procedia Engineering, 69 (2014) 931-936.
[9] BuildIT Construction, Module 8.1: Align scans to CAD – point based alignment with BuildIT Construction. Available on https://knowledge.faro.com/Software/BuildIT/BuildIT_Construction/08.1-Module-Align_Scans_to_CAD_-_Point_Based_Alignment_with_BuildIT_Construction, last updated in 2019.
[10] G. Wolberg, S. Zokai, Robust image registration using log-polar transform, Proceedings 2000 International Conference on Image Processing, 1(2000) 493–496.
[11] M.L. Hetland, The basic principles of metric indexing, Swarm intelligence for multi-objective problems in data mining, (2009)199-232.
[12] Y. Jin, H. Liao, H. Pierson, A multi-resolution framework for automated alignment and error quantification in additive manufacturing. (working paper)
[13] The Stanford 3D Scanning Repository. Available on: http://graphics.stanford.edu/data/3Dscanrep/. Accessed in 2019